HHS Public Access

Author manuscript

J Inherit Metab Dis. Author manuscript; available in PMC 2024 November 01.

Published in final edited form as:

J Inherit Metab Dis. 2023 November ; 46(6): 1195–1205. doi:10.1002/jimd.12679.

Biallelic missense variants in *COG3* cause a congenital disorder of glycosylation with impairment of retrograde vesicular trafficking

Ruizhi Duan[1,*], **Dana Marafi**[1,2,*], **Zhi-Jie Xia**[3,*], **Bobby G. Ng**[3], **Reza Maroofian**[4], **Farhana Taher Sumya**[5], **Ahmed K. Saad**[1,6], **Haowei Du**[1], **Jawid M. Fatih**[1], **Jill V. Hunter**[7], **Hasnaa M. Elbendary**[8], **Shahid M. Baig**[9,10], **Uzma Abdullah**[11], **Zafar Ali**[12], **Stephanie Efthymiou**[4], **David Murphy**[13], **Tadahiro Mitani**[1], **Marjorie A. Withers**[1], **Shalini N. Jhangiani**[14], **Zeynep Coban-Akdemir**[1,15], **Daniel G. Calame**[1,16,17], **Davut Pehlivan**[1,16,17], **Richard A. Gibbs**[1,14], **Jennifer E. Posey**[1], **Henry Houlden**[4], **Vladimir V. Lupashin**[5], **Maha S. Zaki**[8], **Hudson H. Freeze**[3,#], **James R. Lupski**[1,14,16,18,#]

[1]Department of Molecular and Human Genetics, Baylor College of Medicine, Houston, Texas, USA.

[2]Department of Pediatrics, Faculty of Medicine, Kuwait University, Safat, Kuwait.

[3]Human Genetics Program, Sanford Burnham Prebys Medical Discovery Institute, La Jolla, CA, USA

[4]Department of Neuromuscular Disorders, Queen Square Institute of Neurology, University College London, London, UK.

[#]Corresponding authors: Hudson H. Freeze, PhD hudson@sbpdiscovery.org; James R. Lupski MD, PhD, DSc(hon) jlupski@bcm.edu.
[*]Co-first authors

Author Contributions

Conceptualization: R.D., D.Ma., H.H.F., J.R.L.; Clinical data acquisition: D.Ma., R.M., M.S.Z., S.M.B., H.M.E., S.M.B., U.A., and Z.A.; Initial patient sample processing: M.S.Z., J.M.F., M.A.W., A.K.S., and T.M.; Sequencing data curation and annotation: R.D., D.Ma., R.M., A.K.S., S.E., and D.Mu.; Cellular experiments and functional studies: Zj. X., B.G.N., F.T.S., H.H.F., and V.V.L.; Brain MRI analysis and interpretation: J.V.H. and M.S.Z.; Computational support and bioinformatics: H.D., Z.C.A., and D.Mu.; Supervision: J.R.L., H.H.F., R.M., and V.V.L.; Data Visualization: R.D., J.R.L., B.G.N., R.M., F.T.S., H.H.F., and V.V.L.; Funding acquisition: J.R.L., H.H.F., H.Hou., V.V.L., J.E.P., R.A.G., D.G.C., and D.P.; Writing-original draft: R.D., J.R.L., D.Ma., H.H.F., and B.G.N.; Writing-review and editing: All authors.

Conflict of Interest

James R. Lupski has stock ownership in 23andMe, is a paid consultant for Genomics International, and is a co-inventor on multiple United States and European patents related to molecular diagnostics for inherited neuropathies, eye diseases, genomic disorders, and bacterial genomic fingerprinting. The Department of Molecular and Human Genetics at Baylor College of Medicine receives revenue from clinical genetic testing conducted at Baylor Genetics (BG); James R. Lupski serves on the Scientific Advisory Board (SAB) of BG. Ruizhi Duan, Dana Marafi1, Zhi-Jie Xia, Bobby G. Ng, Reza Maroofian, Farhana Taher Sumya, Ahmed K. Saad, Haowei Du, Jawid M. Fatih, Jill V. Hunter, Hasnaa M. Elbendary, Shahid M. Baig, Uzma Abdullah, Zafar Ali, Stephanie Efthymiou, David Murphy, Tadahiro Mitani, Marjorie A. Withers, Shalini N. Jhangiani, Zeynep Coban-Akdemir, Daniel G. Calame, Davut Pehlivan, Richard A. Gibbs, Jennifer E. Posey, Henry Houlden, Vladimir V. Lupashin, Maha S. Zaki and Hudson H. Freeze declare that they have no conflict of interest.

Compliance with Ethics Guidelines

Informed Consent

All procedures followed were in accordance with the ethical standards of the responsible committee on human experimentation (institutional and national) and with the Helsinki Declaration of 1975, as revised in 2000 (5). Informed consent was obtained from all patients for inclusion in the study. This study is approved by the Baylor College of Medicine Institutional Review Board for human subjects research (BCM IRB protocol H-29697) in the United States, and ethical approval GERF33650 in Egypt.
This manuscript does not contain any studies with animal subjects performed by any of the authors.

[5]Department of Physiology and Cell Biology, University of Arkansas for Medical Sciences, Little Rock, Arkansas, USA

[6]Department of Medical Molecular Genetics, Human Genetics and Genome Research Division, National Research Centre, Cairo, Egypt

[7]Department of Pediatric Radiology, Texas Children's Hospital, Baylor College of Medicine, Houston, Texas, USA

[8]Clinical Genetics Department, Human Genetics and Genome Research Institute, National Research Centre, Cairo, Egypt

[9]Department of Biological and Biomedical Sciences, The Aga Khan University, Karachi, Pakistan

[10]Pakistan Science Foundation (PSF), Islamabad, Pakistan

[11]University Institute of Biochemistry and Biotechnology, Pir Mehr Ali Shah Arid Agriculture University, Rawalpindi, Pakistan

[12]Centre for Biotechnology and Microbiology, University of Swat, Swat, Pakistan

[13]Department of Clinical and Movement Neurosciences, UCL Queen Square Institute of Neurology, London, UK

[14]Human Genome Sequencing Center, Baylor College of Medicine, Houston, Texas, USA

[15]Human Genetics Center, Department of Epidemiology, Human Genetics, and Environmental Sciences, School of Public Health, The University of Texas Health Science Center at Houston, Houston, Texas, USA

[16]Texas Children's Hospital, Houston, Texas, USA

[17]Section of Pediatric Neurology and Developmental Neuroscience, Department of Pediatrics, Baylor College of Medicine, Houston, TX, USA

[18]Department of Pediatrics, Baylor College of Medicine, Houston, Texas, 77030, USA

Abstract

Biallelic variants in genes for seven out of eight subunits of the conserved oligomeric Golgi complex (COG) are known to cause recessive congenital disorders of glycosylation (CDG) with variable clinical manifestations. *COG3* encodes a constituent subunit of the COG complex that has not been associated with disease traits in human. Herein, we report two *COG3* homozygous missense variants in four individuals from two unrelated consanguineous families that co-segregated with COG3-CDG. Clinical phenotypes of affected individuals include global developmental delay, severe intellectual disability, microcephaly, epilepsy, facial dysmorphism, and variable neurological findings. Biochemical analysis of serum transferrin from one family showed the loss of a single sialic acid. Western blotting on patient-derived fibroblasts revealed reduced COG3 and COG4. Further experiments showed delayed retrograde vesicular recycling in patient cells. This report adds to the knowledge of the COG-CDG network by providing collective evidence for a COG3-CDG rare disease trait and implicating a likely pathology of the disorder as the perturbation of GA trafficking.

Keywords

Conserved oligomeric Golgi complex (COG); Congenital disorders of glycosylation (CDG); Family-based genomic analysis; AOH/ROH analysis; Retrograde vesicular transport

Introduction

The Golgi apparatus (GA) and endoplasmic reticulum (ER) are part of the endomembrane secretory system of the cell. Trafficking of cargo proteins from the ER to GA involves vesicle carriers that shuttle the cargo to downstream subcellular destinations (i.e., endosomes) or exocytosis. Structurally, GA is assembled from a stack of flattened, membrane-enfolded entities called cisternae, which are laterally interconnected. Coat proteins (COP) are involved in generating the vesicles that maintain bidirectional cargo flow between the ER and Golgi[1]. The polarized, anterograde trafficking flow with COPII carries cargo molecules from ER to GA, whilst in the opposite direction, the COPI-associated retrograde transport shuttles the material from GA back to the ER[2]. This bidirectional equilibrium of the ER-GA network secures those numerous resident proteins, small molecules, and enzymes that follow a balanced allocation over the cisternae. This allows the cargo molecules 'under traffic law' to be progressively and precisely processed and modified[1,2].

Glycosylation is one of the significant post-protein synthesis modifications occurring during ER to GA transport. In this process, the glycan (or oligosaccharide) is built and covalently attached to the cargo macromolecules by an oligosaccharyltransferase complex, which plays an essential role in stabilizing protein structure and function[3]. Genetic disruptions in glycosylation lead to abnormal transport, synthesis, or enzymatic attachment of glycans to proteins and lipids; pathogenic variation of the genes encoding these proteins are known to cause congenital disorders of glycosylation (CDG) in humans[4]. CDGs are a group of rare, genetic metabolic diseases with variable clinical manifestations in several organs and systems. More than 160 CDG types have been identified. A significant fraction of 'CDG genes' (19/140 in omim.org) have been ascribed to the subunits of complexes involving vesicle tethering and scaffolding in intracellular transport[5].

The conserved oligomeric Golgi (COG) complex is one of such vesicle tethering components with eight subunits structurally formed as an octameric hetero-oligomer bridged by two-lobe interaction (Figure 1A)[6,7]. The COG complex is an essential element for intra-GA and retrograde trafficking; aberrations in the COG subunit function can perturb the morphology and function of GA and result in CDG[8]. Biallelic pathogenic variants have been reported in seven out of eight COG subunits resulting in autosomal recessive (AR) CDG-II with variable clinical manifestations[9–15]. Additionally, a recurrent *de novo* monoallelic Gain-of-Function (GoF) allele was reported in *COG4* causing autosomal dominant Saul-Wilson syndrome (MIM # 618150)[16], an osteodysplastic syndrome with short stature and microcephaly. However, no COG3-related disease phenotype has been reported.

Here, we describe two rare, homozygous missense variants mapping to the COG3 N-terminal region in four affected individuals from two unrelated consanguineous families.

These *COG3* variants segregate with an AR CDG and provide further insights into the COG complex structure and function in the cell.

Materials and Methods

Sample recruitment and family-based exome sequencing analysis

Family 1 was recruited into the Baylor-Hopkins Center for Mendelian Genomics now as the BCM-Genomics Research to Elucidate the Genetics of Rare (BCM-GREGoR) disease consortium under BCM Institutional Review Board protocol (H-29697). Family 2 was identified through GeneMatcher[17] and was part of the Queen Square Genomics (QSG) study. Family-based genomics, data analyses, including exome sequencing, rare variant prioritization pipeline and PCR primer sets used for Sanger dideoxy DNA sequencing are detailed in Supplemental Materials. Variant filtering and prioritization were conducted as per the workflow previously described with retrieved allele count collectively from multiple public global and regional databases (Table S1)[18]. Rare candidate variants were further evaluated via *in silico* pathogenicity predictions (Table S1). Genome-wide analysis of absence of heterozygosity (AOH) culled from ES data, and serving as a surrogate measure of runs of homozygosity (ROH), was quantitatively examined from unphased exome data (See Supplemental Materials).

Serum samples from the two affected individuals in family 1 were utilized to perform the biochemical serum transferrin test. The skin biopsies from family 1, BAB13339 (father) and BAB13340 (affected sister) were sampled locally by the referring clinician and transformed into patient-derived fibroblast cell lines by the BCM Tissue Culture Core with consent through the approved IRB protocol listed above. Unaffected control fibroblasts (GM00038, GM03349, and GM09503) were obtained from Coriell Institute for Medical Research (Camden, NJ).

Preparation of patient-derived cell lysates and western blot

To prepare the cell lysates, cells grown on tissue culture dishes were washed three times with phosphate-buffered saline (PBS) and lysed in hot 2 % SDS. Samples were mixed with 6x SDS sample buffer containing β-mercaptoethanol and heated for 10 min at 70 °C. 10 μg of protein was loaded on a Bio-Rad (4–15 %) gradient gel. Proteins were transferred onto nitrocellulose membrane using the Thermo Scientific Pierce G2 Fast Blotter. Membranes were washed in PBS, blocked in Bio-Rad blocking buffer for 20 min, and incubated with primary antibodies for 1 h at room temperature or overnight at 4 °C. Membranes were washed with PBS and incubated with secondary fluorescently tagged antibodies diluted in Bio-Rad blocking buffer for 1 h. Blots were then washed with PBS and imaged using the Odyssey Imaging System. Images were processed using the LI-COR Image Studio software.

For COG subunits, samples were immunoblotted with primary rabbit polyclonal COG subunit antibodies (COG4 provided by Dr. Daniel Ungar, University of York, UK) followed by incubation with secondary Anti-Rabbit HRP (SeraCare, 54500010) antibody. The blots were developed using a SuperSignal West Dura enhanced chemiluminescence

kit (ThermoFisher Scientific, Waltham, MA, USA) according to the manufacturer's instructions. Images were processed using Bio-Rad Image Lab software.

Brefeldin A-induced retrograde transport assay

Fibroblasts from two controls, two subjects, and two other COG-CDG patients were subject to BFA - induced retrograde transport assay as previously described with slight modifications[16]. Briefly, cells were incubated with prewarmed normal growth medium containing 0.25 mg/ml BFA for 0, 5, 10, 15, 22.5, and 30 min at 37 ^{O}C. The incubations were stopped by washing cells with ice-cold PBS three times, and then cells were fixed with 4 % paraformaldehyde for 10 min at room temperature. Cells were permeabilized and stained by Alexa Fluor 488 anti-Giantin antibody (BioLegend, San Diego, CA, USA). The percentage of cells with ER staining was determined at the given time points.

Statistical Analysis

All the western blot images are representative of 3 repeat experiments and those were quantified by densitometry using the LI-COR Image Studio software. Error bars for graphs represent standard deviation. The relative level of all tested proteins was normalized to actin. Statistical analysis was implemented using ANOVA via GraphPad Prism software.

Results

Clinical Report

Family 1.—The elder female affected individual (**BAB13340**) was born by Caesarian section after an uneventful pregnancy and was the third child of consanguineous parents (second cousins once removed) from Egypt (Figure 1B–C). She developed myoclonic seizures at eight months of age and tonic seizures with cyanosis at one year. Both types of seizures remained poorly controlled despite the use of antiepileptic drugs including combinations of levetiracetam, valproate, topiramate, and vigabatrin. At the age of four years and six months, physical examination revealed the following anthropometric measurements: weight of 13 kg (−2.1 SD), height of 101 cm (−0.6 SD), and head circumference of 42.5 cm (−5 SD). She displayed global developmental delay (GDD) due to failure to achieve several motor and cognitive milestones, intellectual disability (ID), and severe microcephaly. Speech was absent, and she failed to respond to external stimuli during the examination. She had dysmorphic facial features including a long face, wide-spaced eyes, squint, prominent nose, long philtrum, thin lips with a V-shaped upper lip, and low-set ears (Figure 1C). Neurological evaluation revealed nystagmus, quadriparesis, bilateral hand tremors, axial and limb hypotonia, and intact deep tendon reflexes. The electroencephalogram (EEG) showed frequent multifocal epileptiform activity, and brain magnetic resonance imaging (MRI) displayed significant cortical volume loss, bilateral symmetric under-opercularization, delayed myelination for age, thin corpus callosum, and mild cerebellar atrophy with a small vermis (Figure 1D–E). The subject had normal 46, XX karyotype. Her fundus examination, and brainstem evoked potentials were normal. Metabolic screening revealed normal urine organic acids, a mildly elevated lactate level (20.4 mg/dL; nml: 4.5 to 19.8 mg/dL), and normal ammonia.

The younger male sibling subject (**BAB13337**) was born by elective Caesarian section after an uneventful pregnancy and was the fourth child in the family (Figure 1F). Similar to his older affected sister, he presented with myoclonic epilepsy at eight months of age without a significant clinical response to valproate and vigabatrin. Physical examination at nine months of age showed a weight of 9 kg (−0.25 SD), a height of 70 cm (−0.5 SD), and significant microcephaly with a head circumference of 40 cm (−4 SD). This subject also displayed features of delayed development but was responsive to stimulation from his surroundings. His facial features included a long face, squint, wide-spaced eyes, long philtrum, and low-set ears (Figure 1F). Neurological examination identified minimal nystagmus, axial and appendicular hypotonia with easily elicited tendon reflexes. EEG uncovered bilateral focal epileptiform discharges in the temporoparietal regions, and brain MRI showed prominent cerebral volume loss, bilateral symmetric under-opercularization, delayed myelination, thin corpus callosum, and a slightly small vermis (Figure 1G–H). He also, similar to his sister, had a mildly elevated serum lactate level (24mg/dl). This subject died at 3 years of age due to aspiration pneumonia.

Family 2.—The first affected male individual (**MR176-01**) was 22 years of age at the last examination. He was born at full term via spontaneous vaginal delivery with no perinatal complications and was the second child of consanguineous parents (first cousins) from Pakistan (Figure 1I–K). Birth measurements were not available. There was no history of neonatal or infantile hypotonia but there was a history of developmental delay. He first sat unsupported at 10 months and walked at 12 months but never attained speech or spoke any word beyond “mom.” There was also a history of regression and aggressive behavior. He had seizures with onset at 2 years of age.

At 22 years of age, he has microcephaly, severe intellectual disability, absent speech, drooling, poor weight gait, muscle wasting, visual impairment, gait impairment and occasional ambulation by crawling. Examination at 22 years of age showed the following anthropometric measurements: height of 146 cm (−4.25 SD for age), weight of 26 kg (−5.1 SD for age) and head circumference of 46 cm (−6 SD for age). He showed abnormal behavior, intermittent crying, subtle dysmorphism and large ears (Figure 1K). He had muscle wasting in the legs (Figure 1M) with spasticity and contractures, symmetric spontaneous movements in all extremities and normally elicited reflexes. Planter reflex was down-going. He was ambulating independently but with a limping gait. The rest of his systemic examination was normal. He never had liver or renal function tests, brain imaging or neurophysiology studies such as electromyogram (EMG) or EEG.

The younger affected individual (**MR176-02)** was a 15-year-old female born via spontaneous vaginal delivery at full term. She was described as having severe intellectual disability, motor impairment, severe visual impairment, and seizures (Figure 1L). Birth measurements were not available. There was no history of infantile hypotonia but similar to her brother, there was a history of developmental delay.

She first sat unsupported at 10 months and walked at 12 months but never attained speech or spoke any word beyond “mom”. There was also a history of regression and aggressive behavior. Her seizures started at 2 years of age. She had a history of severe intellectual

disability, absent speech, poor weight gain, muscle wasting and gait impairment. She died at 15 years of age due to an unknown cause. Detailed examination including anthropometric measurements and neurological assessment was not conducted prior to her death. She never had liver or renal function tests, brain imaging or neurophysiology studies such as EMG or EEG. There was another deceased similarly-affected sister (died at ~15–16 years of age) but no samples were available for further studies. The exact cause of death was unknown, but she was reportedly very weak, bed-ridden and sick at the time of death as her condition was progressively deteriorating. Also, there was an older 33-year-old male with mild intellectual disability and seizures who was heterozygous for the variant.

In summary, the phenotypes of four affected individuals (2 female and 2 male patients) from two unrelated families are described above. A clinical synopsis of the core phenotypic findings include global developmental delay (GDD, 4/4), intellectual disability (ID, 4/4), epilepsy (4/4, with onset from 10 months to 2 years of age), severe microcephaly measured as –4 to −6 SD (3/3), speech impairment (4/4) and facial dysmorphism (4/4). Three of five affected individual (Figure 1) died in childhood or adolescence.

Molecular genetics data of COG3 variants

Family-based ES analysis and Sanger dideoxy DNA sequencing in these two families identified two different rare, homozygous *COG3* missense variant alleles, NM_031431.4: c.124T>C, p.(Ser42Pro) and NM_031431.4: c.109G>C, p.(Asp37His), that co-segregated with the disease phenotypes in each family (Figure 1B and 1I). These two *COG3* missense variants are adjacent to each other and are predicted by conceptual translation to result in the alteration of amino acid residues in one highly conserved alpha-helix structure, conserved from humans to fish (Figure 1J), located adjacent to the N-terminus of COG3. Detailed molecular characteristics of the variants can be found in Table S1.

Genomic evidence of consanguinity and autozygosity in family 1 was revealed by AOH/ROH profiling that identified a similar 37.7 Mb genomic interval of AOH/ROH shared by two affected siblings that encompassed *COG3* (Supplemental materials, Figure S1). A total AOH/ROH of 178.9 Mb in the boy (BAB13337) and 180.1 Mb in the girl (BAB13340) are consistent with a calculated coefficient of consanguinity in the family of the fraction of the genome covered by ROHs (FROH) values 0.036 for the boy (BAB13337) and 0.037 for the girl (BAB13340). Similarly, in family 2, the variant was located within a 29.24Mb interval of AOH/ROH with a total AOH/ROH of 180 Mb in the proband (SYNS-01448) (Supplemental materials, Figure S1).

Biochemical and cellular data of family 1

Biochemical analysis of serum transferrin from two affected individuals in family 1 showed aberrant sialyation with a higher ratio of “tri-sialo” via Mayo Clinic electrospray ionization mass spectrometry (Figure 2A). The damaging effect on COG3 expression caused by the c.124T>C variant was further investigated by western blotting on fibroblasts derived from the female patient (BAB13340) and her father (heterozygous, BAB13339), compared with fibroblasts from three different healthy individuals as controls (GM00038, GM03349, GM09503). The younger affected individual (BAB13337) died before the biopsy

collection was initiated. The COG3 expression in the patient sample (BAB13340) was significantly decreased compared to the controls and the parental sample (Figure 2B–C). Western blotting studies were performed to investigate whether the other three COG Lobe-A subunits (COG1, COG2, and COG4) in the patient sample were also influenced. These investigations revealed that COG4 expression was also significantly decreased in the sample of the affected individual compared with controls and the parental sample, while the expression level of COG1 and COG2 remained unaffected (Figure 2B–C). Comparative analysis of glycoproteins isolated from BAB13339 and BAB13340 fibroblasts using a panel of antibodies to Golgi/endolysosomal resident proteins reveals perturbations in selected glycoproteins and Golgi enzymes, indicating intra-Golgi membrane trafficking defects in COG3-CDG patient (Supplemental materials, Figure S2).

Impairment of retrograde transport from GA to ER is one of the prevalent features in most COG-related CDG. Here, the BFA-induced retrograde transport assay was applied to measure the kinetics of the retrograde transport in the fibroblasts from the patient and parental samples. Figure 2D shows that retrograde transport in the patient's fibroblasts is significantly slower than in the control and parental cells. These functional studies indicate that the *COG3* variant c.124T>C, p.(Ser42Pro) potentially acts as a hypomorphic allele, in which the remnant COG3 may partially sustain its functional performance.

Discussion

The COG protein complex was previously observed under negative-stain electron microscopy showing a specific molecular architecture with a structure consisting of two Y-shaped interacting lobes with four to five spindly helical rods[6,7]. This unique hetero-octamer configuration is conserved from yeast to mammals and is postulated to be remarkably adapted for vesicle capture and fusion[7]. Of note, two amino acid residue alterations described in this study p.(Asp37His) and p.(Ser42Pro) are located within the N-terminal region of COG3. This region of COG3 is known to be important for the subunit-subunit assembly interacting with other COG lobe A components (Figure 1A). We speculate that damaging variants in COG3 may preferentially destabilize the COG lobe A unit, jeopardizing the intracellular bidirectional trafficking equilibrium through the Golgi and resulting in the COG3-CDG phenotype. An alternative etiological hypothesis may attribute organismal pathology to the intracellular interaction of COG3 with a partner protein being weakened by the deleterious variant of *COG3*.

COG4 dosage effects are known to cause a dichotomous outcome of dysfunction in vesicle trafficking[16]. COG4 deficiency due to biallelic deleterious variants also results in compromised GA retrograde transport, with the affected individuals having GDD/ID, epilepsy, microcephaly, and hypotonia with elevated serum transaminases[11,19,20]. Liver function test results were not available in either of our subjects. We hypothesize that reduced COG4 expression due to *COG3* mutation is likely to share the same molecular consequences with COG4 deficiency; thus, it is not surprising that the clinical findings observed in families with *COG3* variants overlap with those observed for COG4-CDG (MIM # 613489) (Table S3). Surprisingly, the opposite phenomenon is observed in patients with Saul-Wilson syndrome (SWILS; MIM #618150), a progeroid syndrome characterized

by skeletal dysplasia and primordial dwarfism, in which the *COG4* GoF alleles abnormally accelerates retrograde transport, leading to a decline of the anterograde transport[16,21].

Our *COG3* variant subject studies further emphasize that the dynamic homeostatic balance and dosage effect of COG4 could be indirectly affected by COG3, or possibly other COG lobe A members due to damaging mutations presumably affecting inter-subunit assembly or stability. Of note, biallelic complete LoF variants in any of four Lobe-A genes have never been reported; we speculate that null alleles may not have been observed potentially due to the lethality of losing both diploid genome copies of the Lobe-A gene during early embryonic stages of development.

Functional studies were limited to one of the two families studied due to biosample availability for family 2. The segregation analysis performed on all eight living members in family 2 provided robust genetic evidence supporting the identified *COG3* homozygous variant as a contributing cause for the observed rare disease trait (Figure 1). Table S2 lists other homozygous candidate variants identified in the affected individuals. Given the consanguinity, homozygosity for several loci is not unexpected. Notably, one homozygous variant in the proband of family 2, *SCN4A*: NM_000334.4: c.91C>T, p.Arg31Trp, is now reported as a variant of unknown significance (VUS) in ClinVar (https://www.ncbi.nlm.nih.gov/clinvar/variation/1303597/). Monoallelic and biallelic variants in *SCN4A* could result in multiple neuromuscular conditions, including recessive inherited congenital myopathy 22A, classic (MIM #620351). Segregation analysis of *SCN4A* VUS variant c.91C>T, p. Arg31Trp shows this variant does not fulfill Mendelian expectations (Figure S3). This VUS variant could potentially contribute to some neuromuscular findings observed in the proband, including muscle wasting in legs, contractures, and impaired gait. Thus, multi-locus pathogenic variation, potentially generated by identity by descent and distributive ROH, could contribute to a blended phenotype[22,23]. Nevertheless, these genetic observations in this family do not rule out the possibility that other factors, including variant alleles detected in the proband-ES at other loci, or variants not detected in proband-only ES might contribute to the disease phenotype observed in the proband[22,23].

Family-based genomics and rare variant analyses expand our knowledge of glycobiology, propel the precise molecular diagnosis of CDG, and facilitate novel gene discovery in this field[4]. Biochemical analysis and functional examination on the specimens from affected subjects can further validate the candidate variant gleaned from genomic and genetic analyses, and perhaps provide new insights of mutational mechanisms in disease biology[4]. Future studies to identify other variants and construct an allelic series may enable further insights into the functional biology of this COG3 subunit; systematic deep clinical phenotyping might uncover a recognizable pattern of dysmorphology.

This study adds to the knowledgebase of the COG-related glycosylation disease network by providing evidence for COG3-CDG via family-based genomic analysis and deep clinical, molecular biological, biochemical and cellular phenotyping with international collaborative data sharing. Functional validations unveiled reduced expression of both COG3 and COG4, driving a delayed retrograde transport from GA to ER, further addressing the mutational

vulnerability of the inter-subunit interaction region at the N-termini of the four subunit Lobe A of COG.

Supplementary Material

Refer to Web version on PubMed Central for supplementary material.

Acknowledgments

We thank the families for their participation in the study.

Funding Statement

This study was supported in part by the U.S. National Human Genome Research Institute (NHGRI), and National Heart Lung and Blood Institute (NHLBI) to the Baylor-Hopkins Center for Mendelian Genomics (BHCMG, UM1 HG006542) and NHGRI Baylor College of Medicine Genomics Research Elucidates Genetics of Rare (BCM-GREGoR; U01 HG011758). Also supported in part by U.S. National Institute of Neurological Disorders and Stroke (NINDS) (R35NS105078), the Muscular Dystrophy Association (MDA; 512848), and Spastic Paraplegia Foundation (SPF) to J.R.L. Support was provided to H.H.F. and B.G.N. by The Rocket Fund and R01DK099551. D.M. was supported by a Medical Genetics Research Fellowship Program through the United States National Institute of Health (T32 GM007526-42). J.E.P. was supported by NHGRI K08 HG008986. D.P. is supported by the International Rett Syndrome Foundation (IRSF grant #3701-1). D.G.C is supported by Muscular Dystrophy Association Development Grant 873841 (https://doi.org/10.55762/pc.gr.147552), Chao Physician-Scientist Award, and U.S. National Institute of General Medical Sciences (NIGMS) 5T32GM007526 Medical Genetics Research Program. V.V.L was supported by NIGMS R01083144. M.S.Z was supported by Egypt STDF-33650.

Data Availability

All data described in this study including raw sequencing data and clinical data can be de-identified and are available upon request to the corresponding authors.

References

1. Park S-Y, Yang J-S, Schmider AB, Soberman RJ, Hsu VW. Coordinated regulation of bidirectional COPI transport at the Golgi by CDC42. Nature. 2015;521(7553):529–532. doi:10.1038/nature14457 [PubMed: 25945738]
2. Nakano A Polarized transport in the Golgi apparatus. Nature. 2015;521(7553):427–428. doi:10.1038/nature14521 [PubMed: 25945742]
3. Reily C, Stewart TJ, Renfrow MB, Novak J. Glycosylation in health and disease. Nat Rev Nephrol. 2019;15(6):346–366. doi:10.1038/s41581-019-0129-4 [PubMed: 30858582]
4. Freeze HH, Chong JX, Bamshad MJ, Ng BG. Solving glycosylation disorders: Fundamental approaches reveal complicated pathways. Am J Hum Genet. 2014;94(2):161–175. doi:10.1016/j.ajhg.2013.10.024 [PubMed: 24507773]
5. Climer LK, Dobretsov M, Lupashin V. Defects in the COG complex and COG-related trafficking regulators affect neuronal Golgi function. Front Neurosci. 2015;9(OCT):1–9. doi:10.3389/fnins.2015.00405 [PubMed: 25653585]
6. Ha JY, Chou HT, Ungar D, Yip CK, Walz T, Hughson FM. Molecular architecture of the complete COG tethering complex. Nat Struct Mol Biol. 2016;23(8):758–760. doi:10.1038/nsmb.3263 [PubMed: 27428773]
7. Lees JA, Yip CK, Walz T, Hughson FM. Molecular organization of the COG vesicle tethering complex. Nat Struct Mol Biol. 2010;17(11):1292–1297. doi:10.1038/nsmb.1917 [PubMed: 20972446]
8. D'Souza Z, Taher FS, Lupashin VV. Golgi inCOGnito: From vesicle tethering to human disease. Biochim Biophys Acta - Gen Subj. 2020;1864(11). doi:10.1016/j.bbagen.2020.129694

9. Foulquier F, Vasile E, Schollen E, et al. Conserved oligomeric Golgi complex subunit 1 deficiency reveals a previously uncharacterized congenital disorder of glycosylation type II. Proc Natl Acad Sci U S A. 2006;103(10):3764–3769. doi:10.1073/pnas.0507685103 [PubMed: 16537452]
10. Kodera H, Ando N, Yuasa I, et al. Mutations in *COG2* encoding a subunit of the conserved oligomeric golgi complex cause a congenital disorder of glycosylation. Clin Genet. 2015;87(5):455–460. doi:10.1111/cge.12417 [PubMed: 24784932]
11. Reynders E, Foulquier F, Teles EL, et al. Golgi function and dysfunction in the first COG4-deficient CDG type II patient. Hum Mol Genet. 2009;18(17):3244–3256. doi:10.1093/hmg/ddp262 [PubMed: 19494034]
12. Paesold-Burda P, Maag C, Troxler H, et al. Deficiency in COG5 causes a moderate form of congenital disorders of glycosylation. Hum Mol Genet. 2009;18(22):4350–4356. doi:10.1093/hmg/ddp389 [PubMed: 19690088]
13. Lübbehusen J, Thiel C, Rind N, et al. Fatal outcome due to deficiency of subunit 6 of the conserved oligomeric Golgi complex leading to a new type of congenital disorders of glycosylation. Hum Mol Genet. 2010;19(18):3623–3633. doi:10.1093/hmg/ddq278 [PubMed: 20605848]
14. Wu X, Steet RA, Bohorov O, et al. Mutation of the COG complex subunit gene *COG7* causes a lethal congenital disorder. Nat Med. 2004;10(5):518–523. doi:10.1038/nm1041 [PubMed: 15107842]
15. Kranz C, Ng BG, Sun L, et al. COG8 deficiency causes new congenital disorder of glycosylation type IIh. Hum Mol Genet. 2007;16(7):731–741. doi:10.1093/hmg/ddm028 [PubMed: 17331980]
16. Ferreira CR, Xia ZJ, Clément A, et al. A Recurrent De Novo Heterozygous *COG4* Substitution Leads to Saul-Wilson Syndrome, Disrupted Vesicular Trafficking, and Altered Proteoglycan Glycosylation. Am J Hum Genet. 2018;103(4):553–567. doi:10.1016/j.ajhg.2018.09.003 [PubMed: 30290151]
17. Sobreira N, Schiettecatte F, Valle D, Hamosh A. GeneMatcher: a matching tool for connecting investigators with an interest in the same gene. Hum Mutat. 2015;36(10):928–930. doi:10.1002/humu.22844 [PubMed: 26220891]
18. Eldomery MK, Coban-Akdemir Z, Harel T, et al. Lessons learned from additional research analyses of unsolved clinical exome cases. Genome Med. 2017;9(1):26. doi:10.1186/s13073-017-0412-6 [PubMed: 28327206]
19. Ng BG, Sharma V, Sun L, et al. Identification of the first COG–CDG patient of Indian origin. Mol Genet Metab. 2011;102(3):364–367. doi:10.1016/j.ymgme.2010.11.161 [PubMed: 21185756]
20. Miura Y, Tay SKH, Aw MM, Eklund EA, Freeze HH. Clinical and Biochemical Characterization of a Patient with Congenital Disorder of Glycosylation (CDG) IIx. J Pediatr. 2005;147(6):851–853. doi:10.1016/j.jpeds.2005.07.038 [PubMed: 16356446]
21. Xia ZJ, Zeng XXI, Tambe M, Ng BG, Dong PDS, Freeze HH. A Dominant Heterozygous Mutation in *COG4* Causes Saul–Wilson Syndrome, a Primordial Dwarfism, and Disrupts Zebrafish Development via Wnt Signaling. Front Cell Dev Biol. 2021;9(September). doi:10.3389/fcell.2021.720688
22. Karaca E, Posey JE, Coban Akdemir Z, et al. Phenotypic expansion illuminates multilocus pathogenic variation. Genet Med Off J Am Coll Med Genet. 2018;20(12):1528–1537. doi:10.1038/gim.2018.33
23. Posey JE, Harel T, Liu P, et al. Resolution of Disease Phenotypes Resulting from Multilocus Genomic Variation. N Engl J Med. 2017;376(1):21–31. doi:10.1056/nejmoa1516767 [PubMed: 27959697]

Synopsis (one sentence):

We described biallelic *COG3* variants in association with a congenital disorder of glycosylation in two unrelated consanguineous families; functional studies suggest reduced protein expression or stability with consequent Golgi trafficking perturbations.

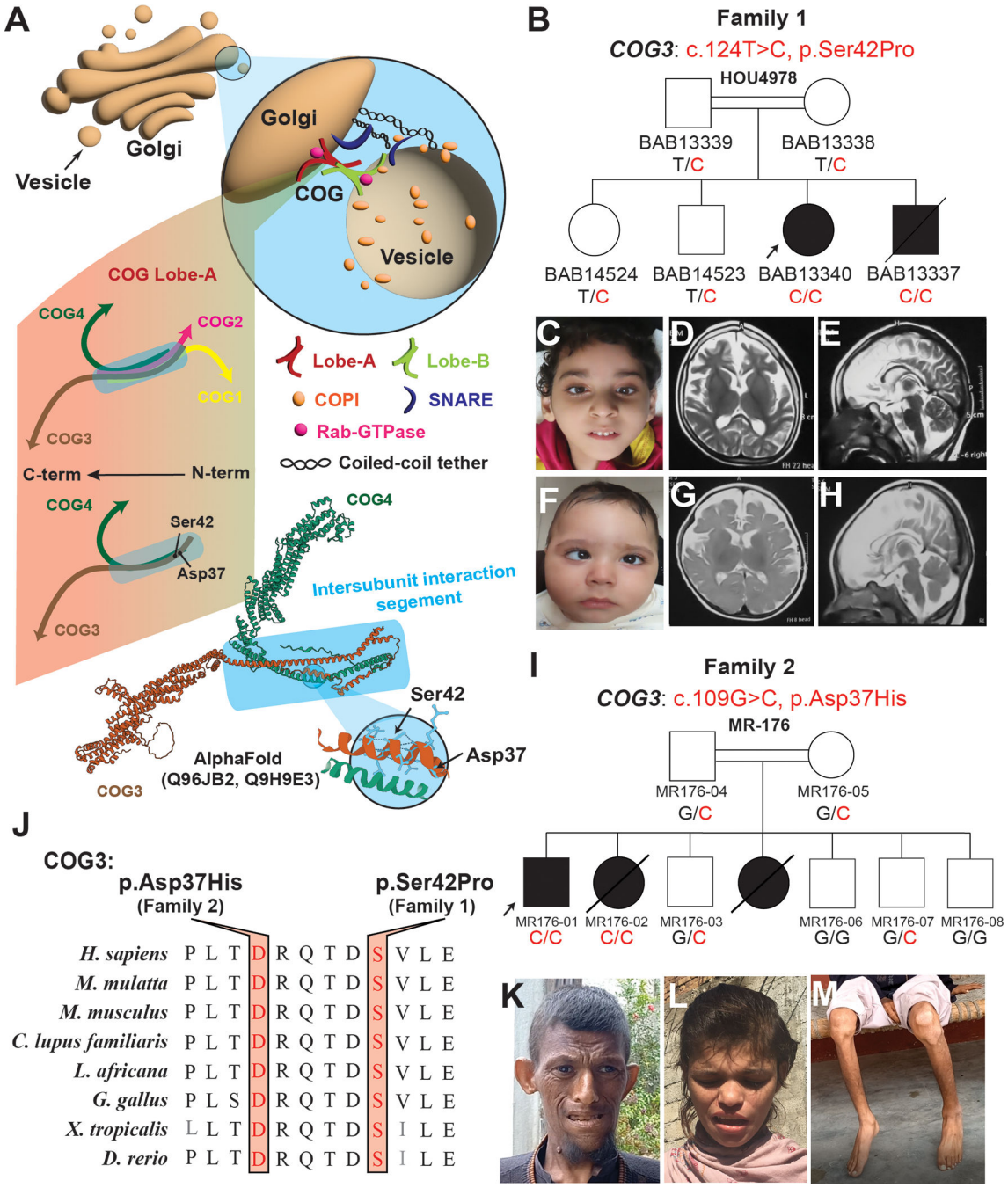

Figure 1.

Comprehensive illustration, familial pedigree, clinical photographs and genetic findings of the identified homozygous variant in *COG3*

(A) An illustrative graph briefly describes the of COG-mediated vesicular tethering. During the early phase of membrane fusion, partially coated vesicle can be captured by the of multisubunit tethering machinery including the COG complex (as the recognitional bridge), soluble N-ethylmaleimide-sensitive factor attachment protein receptor (SNARE) and Rab GTPases. Structural diagram of COG Lobe-A was adapted from the publication (Lee et

al, Nat Struct Mol Biol, 2010). The reported variant p.(Ser42Pro) resides in the COG3 N-terminus, a long segment of α-helix presumably involved quaternary interactions with the other three subunits (shaded by blue rectangle in the diagram). Location of the variant was highlighted by 3D protein structural modeling of COG3 and COG4 obtained from AlphaFold Protein Structure Database (https://alphafold.ebi.ac.uk/). **(B)** Pedigree and allelic information with the segregation of the missense variant *COG3* [NM_031431.4: c.124T>C, p.(Ser42Pro)] in the family 1 (HOU4978).

(C) Clinical photograph of the female affected individual BAB13440 showing mild facial dysmorphism. **(D-E)** Brain MRI (Axial and midsagittal T2 weighted imaging, respectively) of BAB13340 at 5 years of age showing mild right posterior plagiocephaly, generous CSF spaces, wide interhemispheric fissure, significant cerebral volume loss, bilateral symmetric under-opercularization, delayed myelination for age, thinning of corpus callosum, prominent supratentorial and fourth ventricles, and mild superior vermian hypoplasia. The findings reflect a more severe supratentorial than infratentorial involvement. **(F)** Clinical photograph of the deceased individual BAB13337 showing mild facial dysmorphism and strabismus **(G-H)** Brain MRI (Axial and midsagittal T2 weight imaging, respectively) BAB13337 at 4 months of age showing right posterior plagiocephaly, generous CSF spaces, prominent cerebral volume loss, bilateral symmetric under-opercularization, delayed myelination for age, thinning of corpus callosum, normal supratentorial ventricular system with large 4th ventricle, and very mild superior vermian hypoplasia. **(I)** Pedigree and allelic information with the segregation of the missense variant *COG3* [NM_031431.4: c.109G>C, p.(Asp37His)] in family 2 (MR-176). Note: the there are two deceased affected female individuals in this family. The elder one (SYNS-01449) was confirmed harboring the homozygous variant of *COG3* with phenotype information reported. While the genotype and phenotype information of the younger deceased individual (female, affected) is not available. **(J)** The altered amino acids and other adjacent residues are evolutionarily conserved. **(K)** A clinical photograph of the proband SYNS-01448 shows subtle facial dysmorphism. **(L)** A photograph of the deceased female affected individual SYNS-01449 shows a similar facial feature. **(M)** A photograph of the proband SYNS-01448 shows muscle wasting in the legs.

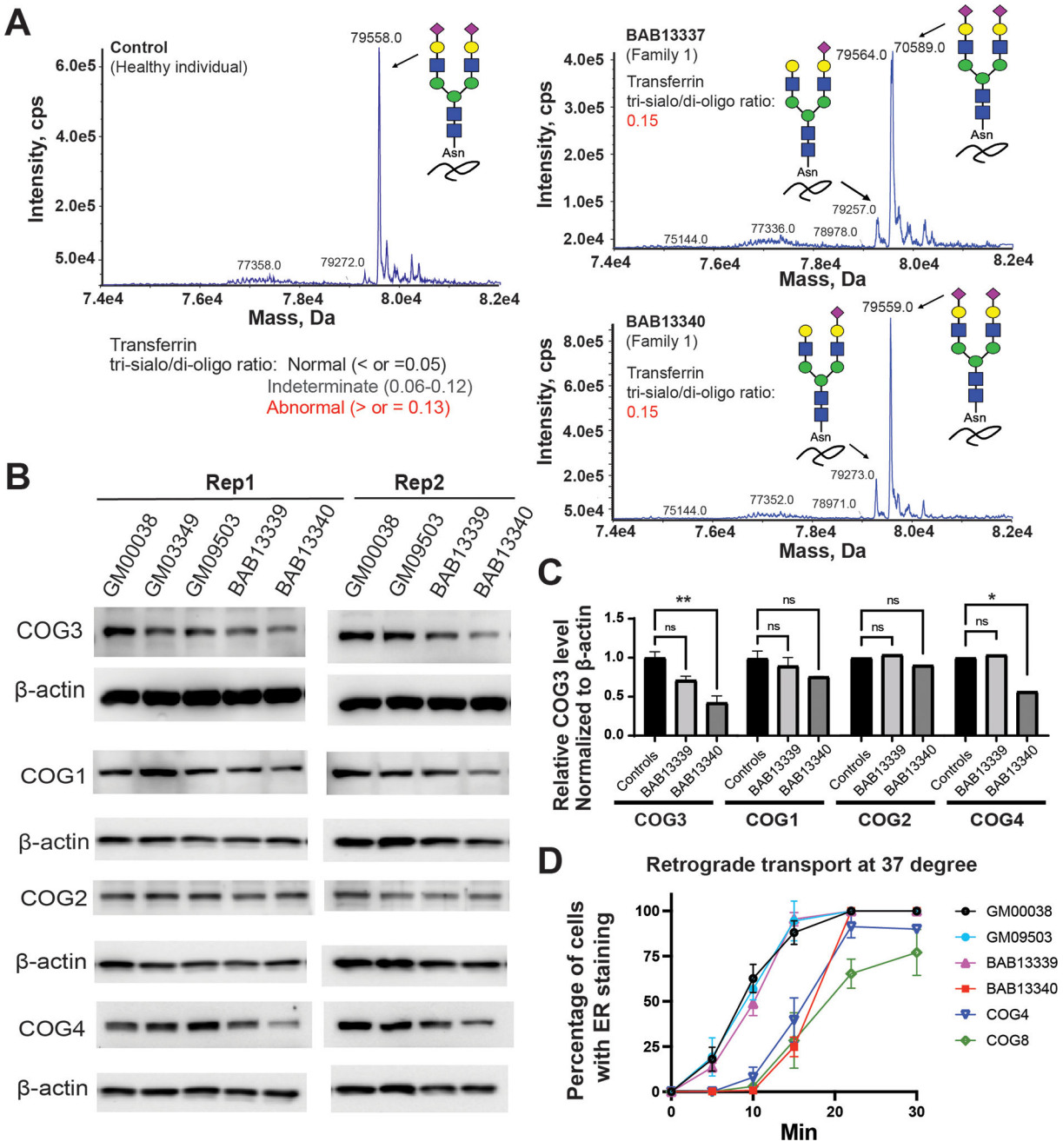

Figure 2.

Reduced expression of COG3 and COG4 with delayed retrograde trafficking

(A) Biochemical analysis on serum transferrin from two affected individuals in family 1 showed aberrant sialyation with a higher ratio of 'tri-sialo/di-oligo' compared with a healthy individual control via MAYO electrospray ionization mass spectrometry. **(B-C)** Western blot images of COG3, COG1, COG2 and COG4 abundance in unaffected control, BAB13339, and BAB13340 fibroblasts. Relative COG3 level was normalized to β-actin, the internal loading control of Western blotting. The experiment was performed in duplicate with similar results. The reduction of COG3 was seen in BAB13339 by more than 50% compared

to unaffected controls. A significantly reduced COG4 was seen in BAB13339 compared to unaffected controls. The experiment was performed in duplicate with similar results. Unpaired two-tailed t-test was used. *, $p<0.05$; **, $p<0.01$. **(D)** BFA-induced retrograde transport of Giantin in unaffected controls, BAB13339, BAB13340, and other COG-CDG individuals' fibroblasts. The percentage of ER staining pattern of Giantin was calculated at 0, 5, 10, 15, 22.5, and 30 min with BFA treatment in fixed samples. 80–100 cells were counted at each time point. Experiments were done in triplicate. COG4, LoF COG4-CDG individual's fibroblast. COG8, COG8-CDG individual's fibroblast.